ISCI, Volume *20*

Supplemental Information

Skin Patterning in Psoriasis by Spatial Interactions between Pathogenic Cytokines

Lee Ringham, Przemyslaw Prusinkiewicz, and Robert Gniadecki

Transparent Methods

Source of information on the patterns of psoriatic lesions

Patterns of skin lesions in psoriasis have been reviewed using the "(psoriasis AND clinical AND (pattern OR shapes)) OR (clinical spectrum AND psoriasis)" search phrases in PubMed. We retrieved 715 papers and after reviewing the titles and abstracts we selected 40 relevant papers (Ayala, 2007; Baker, 1971; Balato et al., 2009; Beylot et al., 1979; Buxton, 1987; Champion, 1986; Chau et al., 2017; Christophers, 2001; Cordoro, 2008; Di Meglio et al., 2014; Fernandes et al., 2011; Gropper, 2001; Hernández-Vásquez et al., 2017; Hodge and Comaish, 1977; Jablonska et al., 2000; Kumar et al., 1995; Lal, 1966; Lebwohl, 2003; Magro and Crowson, 1997; Meier and Sheth, 2009; Melski et al., 1983; Menter and Barker, 1991; M G et al., 2013; Mitchell, 1962; Morris et al., 2001; Naldi and Gambini, 2007; de Oliveira et al., 2010; Picciani et al., 2017; Rasmussen, 1986; Raychaudhuri et al., 2014; Reich et al., 2009; Saleh and Tanner, 2018; Schön et al., 2005; Seneschal et al., 2012; Stankier, 1974; Stern, 1997; Talwar et al., 1995; Whyte and Baughman, 1964; Wollenberg and Eames, 2011; Ziemer et al., 2009). We also reviewed 482 clinical photographs of psoriasis in the database of the Department of Dermatology, University of Copenhagen and the Division of Dermatology, University of Alberta. We have excluded linear psoriasis, psoriatic erythroderma, and guttate psoriasis from our analyses. The linear pattern is the isomorphic (Köbner) response to trauma and does not emerge spontaneously (Melski et al., 1983). Erythroderma manifests itself as diffuse redness and inflammation of the entire skin, and thus lacks features of a pattern. Guttate psoriasis is considered to be a separate clinical type of the disease (Rasmussen, 1986; Raychaudhuri et al., 2014; Whyte and Baughman, 1964), but it is not distinguishable from papular or nummular psoriasis based on lesion morphology.

Computer model

The progress and treatment of the disease was simulated by numerically solving the initial value problem for the reaction-diffusion equations using the forward Euler method. Simulations have been implemented using a custom reaction-diffusion modeling program written in C++ within the Windows Visual Studio programming environment. To facilitate interactive exploration of the models and their parameters, computation has been accelerated (carried out in a parallel fashion) on a Nvidia GeForce GTX 850M Graphical Processing Unit, with arrays representing the previous and current state of the simulation in each step implemented as textures (Dematté and Prandi, 2010; Harris et al., 2005). The textures used in all simulations had a resolution of 500 x 500 texels, with each texel representing a sample point of a discretized patch of the skin. Parameters of individual simulations are collected in Table S1. We assumed Neumann boundary conditions set to 0, i.e., no diffusion of activator A and substrate S across the boundary. The initial activator concentration a was set to 0 in each texel except for 50 seed spots, placed randomly across the domain. Each spot was represented by a 3x3 array of texels with a concentration of 0.5 (See Table S3 for the minimum values). The initial concentration of the substrate s was 1.0 everywhere. All concentrations were represented with 32-bit floating point accuracy.

Supplementary Equations

To show that the results obtained for the two-substance system in Fig. 2B also hold for the three-substance system in Fig. 2A, we have constructed a simulation model corresponding directly to Fig. 2A. The equations have the form:

$$\frac{\partial[TNF\alpha]}{\partial t} = \rho_{[TNF\alpha]0} - \mu_{[TNF\alpha]}[TNF\alpha] + \eta[IL17] - k[TNF\alpha]^2[IL23] + D_{[TNF\alpha]}\nabla^2[TNF\alpha]$$

$$\frac{\partial[IL17]}{\partial t} = \rho_{[IL17]0} - \mu_{[IL17]}[IL17] + k[TNF\alpha]^2[IL23] + D_{[IL17]}\nabla^2 2[IL17]$$

$$\frac{\partial[IL23]}{\partial t} = \rho_{[IL23]0} - \mu_{[IL23]}[IL23] - k[TNF\alpha]^2[IL23] + D_{[IL23]}\nabla^2[IL23]$$

Parameter values resulting in the different pattern classes shown in Fig. 4 are collected in Table S3.

Supplementary Tables and Figures

Molecule	***MW* [kDa]**	***D*$_{tiss}$ [µm^2/s]**
TNFα	26	154.4
IL17	35	123.6
IL23	54.1	89.1

Table S1. Diffusion coefficients for the three cytokines involved in our model using the empirical formula $D_{tiss} = 1.778 \times 10^{-4} \times MW^{-0.75}$ (Swabb et al., 1974) (Equation F in their paper; MW = molecular weight), related to Figure 2. The actual rates of macromolecule transport in a tissue may differ from these estimates, as other factors may also play a role. These include convection, which may run in the direction opposite to the concentration-gradient-driven diffusion (Swabb et al., 1974), and cell proliferation, which may be relevant to the transport of cytokines otherwise mostly confined to their mother cells.

Name	Papular	Small Plaque	Large Plaque	Annular	Rosette	Reniform
$\rho_{s0}=\mu_s$	0.046	0.084	0.091	0.001	0.009	0.011
μ_a *(before treatment)*	0.116	0.141	0.148	0.028	0.056	0.057
μ_a *(during treatment)*	0.120	0.1467	0.153	0.04	0.0625	0.065
maxSteps	12,620	14,000	143,000	4,500	3,900	15,500
treatSteps	12,000	12,000	140,000	1,700	2,700	13,000

Table S2. Parameter values used to generate the six classes of psoriasis plaque patterns, related to Fig. 4. In all simulations $k = 1$, $\rho_{a0} = 0$, $D_a = 0.25$, and $D_s = 0.5$. Simulations were carried out using forward Euler methods with time step $dt = 0.4$ for *maxSteps* iterations, with the treatment starting after *treatSteps* iterations.

Name	Papular	Small Plaque	Large Plaque	Annular	Rosette	Reniform
ρ_{s0}	[0.04510, 0.04705]	[0.08375, 0.15000]	[0.09060, 0.09110]	[0.00075, 0.00285]	[0.00875, 0.00910]	[0.01085, 0.01112]
ρ_{a0}	[0.00000, 0.00075]	[0.00000, 0.00525]	[0.00000, 0.00002]	[0.00000, 0.00022]	[0.00000, 0.00015]	[0.00000, 0.00008]
μ_s	[0.04435, 0.04725]	[0.03475, 0.08475]	[0.09085, 0.09175]	[0.00000, 0.00125]	[0.00875, 0.00910]	[0.01085, 0.01120]
μ_a	[0.11265, 0.11899]	[0.10000, 0.14180]	[0.14785, 0.14870]	[0.01500, 0.03500]	[0.05360, 0.05650]	[0.05620, 0.05750]
D_s	[0.46000, 0.57500]	[0.42500, 0.80000]	[0.46100, 0.50500]	[0.00000, 1.05000]	[0.47500, 0.52500]	[0.42500, 0.61500]
D_a	[0.22000, 0.27000]	[0.17500, 0.29000]	[0.24500, 0.27000]	[0.15000, 0.75000]	[0.23500, 0.27500]	[0.22500, 0.28500]
k	[0.95900, 1.05000]	[0.98800, 1.60000]	[0.99000, 1.00200]	[0.75000, 1.35000]	[0.98500, 1.06500]	[0.97500, 1.01500]

Table S3. Ranges of parameter values resulting in pattern formation, related to Figure 4. For each varied parameter all remaining values are as in Table S2.

Pattern	A	B	C	D1	D2	D3
Minimum initial concentration of the activator at the spots	0.208	0.244	0.256	0.088	0.126	0.127

Table S4. Minimum concentrations of activator A needed to initiate the formation of patterns, related to Figure 4.

Parameter	Papular	Small Plaque	Large Plaque	Annular	Rosette	Reniform
$\mu_{[IL23]} = \rho_{[IL23]0}$	0.04	0.045	0.055	0.001	0.009	0.011
$\mu_{[TNF\alpha]}$*(before treatment)*	0.103	0.103	.115	0.028	0.055	0.054
$\mu_{[TNF\alpha]}$ *(during treatment)*	0.107	0.1087	0.12	0.04	0.0615	0.062
maxSteps	13,000	14,000	143,000	4,500	3,900	15,500
treatSteps	12,000	12,000	140,000	1,700	2,700	13,000

Table S5. Parameter values for generating the six classes of psoriasis plaque patterns using the three-substance model, related to Figure 4. In all simulations $k = 1, \eta = 2, \rho_{[TNF\alpha]0} = \rho_{[IL17]0} = 0$, $\mu_{[IL17]} = 1$, $D_{[IL23]} = 0.5, D_{[TNF\alpha]} = D_{[IL17]} = 0.25$. Simulations were carried out using forward Euler methods with time step *dt* = 0.4 for *maxSteps* iterations, with the treatment starting after *treatSteps* iterations.

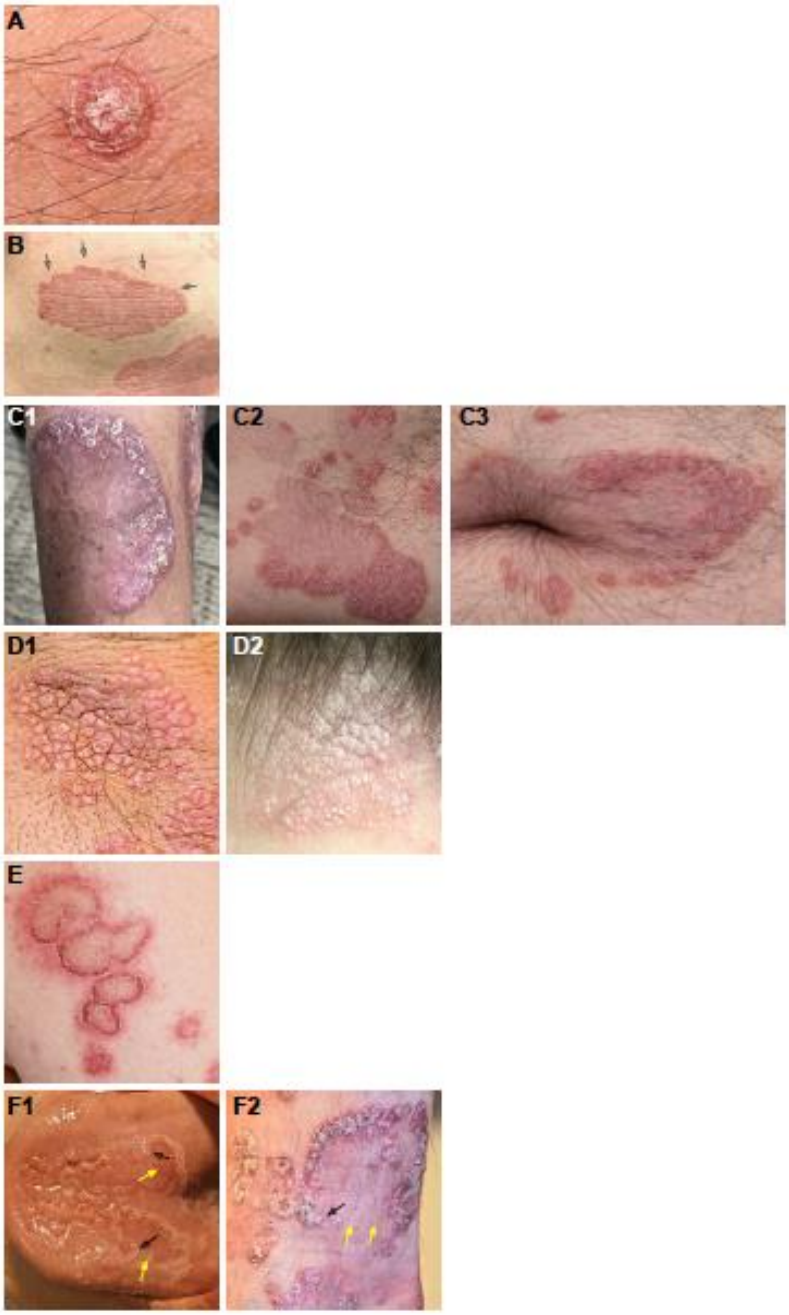

Figure S1. Morphological details of different patterns of skin lesions in psoriasis, related to Figure 1. **A:** Psoriatic papule. Note that the scale and the thickness is accentuated in the center, indicating that the inflammatory reaction is most intense in the center of the lesion. **B:** Mature psoriasis plaque showing more activity in the periphery (open arrowheads) than in the center. **C:** Resolution of psoriatic plaques during treatment. Note central clearing of the plaque and residual peripheral activity producing a circinate pattern. **D:** Internal patterning of the plaques showing polygonal faceting. **E**: Merging circinate lesions. Annular plaques merge into polycyclic structures with clearance of the cross-sectioning parts of the lesions (open arrowhead). **F:** Reniform pattern on mucosal surface of the tongue (lingua geographica, left) and on the skin (right). Yellow solid arrows show the notched part of the lesion, black open arrowheads show the curled part at the notch.

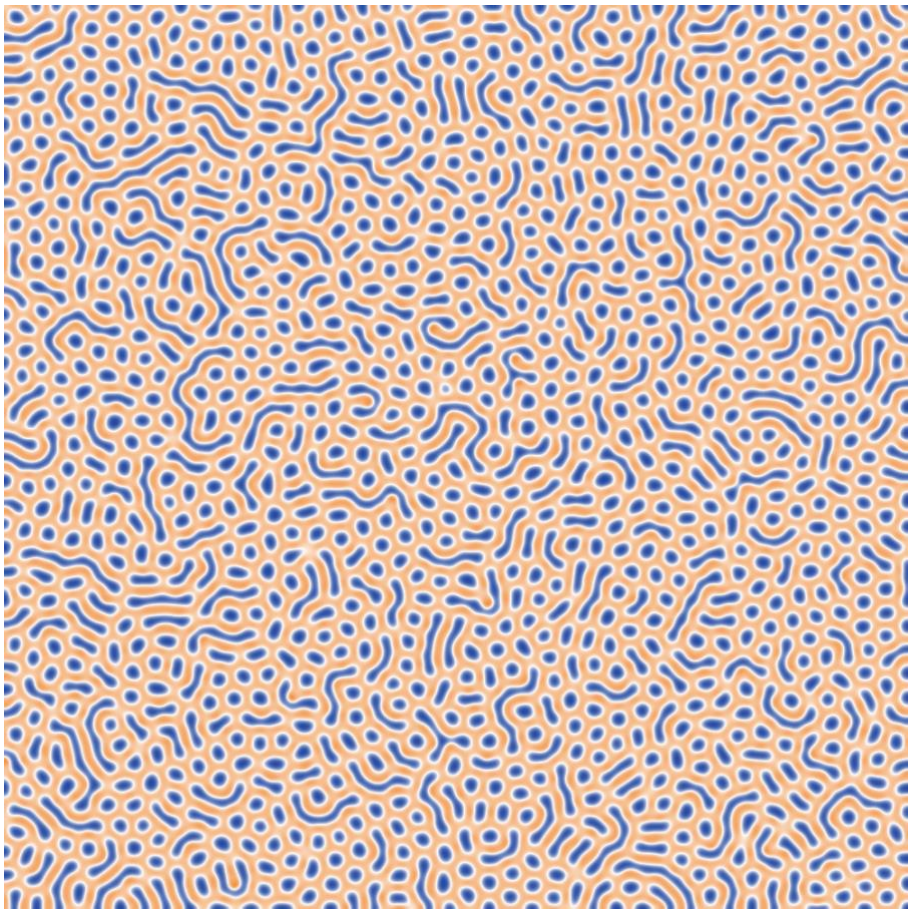

Figure S2. Example of a pattern generated de novo using the Gray-Scott model (Equation 2) after 6000 iterations, related to Figure 3. The concentration is visualized from blue to orange. Parameter values: $f = 0.042, c = 0.06, D_a = 0.25, D_s = 0.5, dt = 1$. The initial conditions are a homogenous distribution everywhere, with the addition of a small amount of noise: a=0.22557, s=0.45219±0.000001.

Supplementary Movies

Movie S1. Simulated development and response to treatment of papular lesions, related to Figure 4

Movie S2. Simulated development and response to treatment of small plaque / nummular lesions, related to Figure 4

Movie S3. Simulated development and response to treatment of large plaque lesions, related to Figure 4

Movie S4. Simulated development and response to treatment of annular lesions, related to Figure 4

Movie S5. Simulated development and response to treatment of rosette lesions, related to Figure 4

Movie S6. Simulated development and response to treatment of reniform lesions, related to Figure 4

References for Supplemental Information

Ayala, F. (2007). Clinical presentation of psoriasis. Reumatismo *59 Suppl 1*, 40–45.

Baker, H. (1971). Psoriasis--clinical features. Br. Med. J. *3*, 231–233.

Balato, N., Di Costanzo, L., and Balato, A. (2009). Differential diagnosis of psoriasis. J. Rheumatol. Suppl. *83*, 24–25.

Beylot, C., Puissant, A., Bioulac, P., Saurat, J.H., Pringuet, R., and Doutre, M.S. (1979). Particular clinical features of psoriasis in infants and chidren. Acta Derm. Venereol. Suppl. *87*, 95–97.

Buxton, P.K. (1987). ABC of Dermatology. Psoriasis. Br. Med. J. *295*, 904–906.

Champion, R.H. (1986). Psoriasis. Br. Med. J. *292*, 1693–1696.

Chau, T., Parsi, K.K., Ogawa, T., Kiuru, M., Konia, T., Li, C.-S., and Fung, M.A. (2017). Psoriasis or not? Review of 51 clinically confirmed cases reveals an expanded histopathologic spectrum of psoriasis. J. Cutan. Pathol. *44*, 1018–1026.

Christophers, E. (2001). Psoriasis--epidemiology and clinical spectrum. Clin. Exp. Dermatol. *26*, 314–320.

Cordoro, K.M. (2008). Management of childhood psoriasis. Adv. Dermatol. *24*, 125–169.

Dematté, L., and Prandi, D. (2010). GPU computing for systems biology. Brief. Bioinform. *11*, 323–333.

Di Meglio, P., Villanova, F., and Nestle, F.O. (2014). Psoriasis. Cold Spring Harb. Perspect. Med. *4*.

Fernandes, S., Pinto, G.M., and Cardoso, J. (2011). Particular clinical presentations of psoriasis in HIV patients. Int. J. STD AIDS *22*, 653–654.

Gropper, C.A. (2001). An approach to clinical dermatologic diagnosis based on morphologic reaction patterns. Clin. Cornerstone *4*, 1–14.

Harris, M.J., Coombe, G., Scheuermann, T., and Lastra, A. (2005). Physically-based visual simulation on graphics hardware. In ACM SIGGRAPH 2005 Courses on - SIGGRAPH '05.

Hernández-Vásquez, A., Molinari, L., Larrea, N., and Ciapponi, A. (2017). Psoriasis in Latin America and the Caribbean: a systematic review. J. Eur. Acad. Dermatol. Venereol. *31*, 1991–1998.

Hodge, L., and Comaish, J.S. (1977). Psoriasis: current concepts in management. Drugs *13*, 288–296.

Jablonska, S., Blaszczyk, M., and Kozlowska, A. (2000). Erythema gyratum repens-like psoriasis. Int. J. Dermatol. *39*, 695–697.

Kumar, B., Kaur, I., and Thami, G.P. (1995). Plantar psoriasis: clinical correlation of lesion pattern to weight bearing. Acta Derm. Venereol. *75*, 157–158.

Lal, S. (1966). Clinical Pattern of Psoriasis in Punjab. Indian J. Dermatol. Venereol. Leprol. *32*, 5–8.

Lebwohl, M. (2003). Psoriasis. Lancet *361*, 1197–1204.

Magro, C.M., and Crowson, A.N. (1997). The clinical and histomorphological features of pityriasis rubra pilaris. A comparative analysis with psoriasis. J. Cutan. Pathol. *24*, 416–424.

Meier, M., and Sheth, P.B. (2009). Clinical spectrum and severity of psoriasis. Curr. Probl. Dermatol. *38*, 1–20.

Melski, J.W., Bernhard, J.D., and Stern, R.S. (1983). The Koebner (isomorphic) response in psoriasis. Associations with early age at onset and multiple previous therapies. Arch. Dermatol. *119*, 655–659.

Menter, A., and Barker, J.N. (1991). Psoriasis in practice. Lancet *338*, 231–234.

M G, G., Talwar, A., Kumar B C, S., M, R., A S, N., and H B, M. (2013). A clinical and epidemiological study of psoriasis and its association with various biochemical parameters in newly diagnosed cases. J. Clin. Diagn. Res. *7*, 2901–2903.

Mitchell, J.C. (1962). The Distribution Patterns of Psoriasis: Observations on the Koebner Response. Can. Med. Assoc. J. *87*, 1271–1274.

Morris, A., Rogers, M., Fischer, G., and Williams, K. (2001). Childhood psoriasis: a clinical review of 1262 cases. Pediatr. Dermatol. *18*, 188–198.

Naldi, L., and Gambini, D. (2007). The clinical spectrum of psoriasis. Clin. Dermatol. *25*, 510–518.

de Oliveira, S.T., Maragno, L., Arnone, M., Fonseca Takahashi, M.D., and Romiti, R. (2010). Generalized pustular psoriasis in childhood. Pediatr. Dermatol. *27*, 349–354.

Picciani, B., Santos, V. de C., Teixeira-Souza, T., Izahias, L.M., Curty, Á., Avelleira, J.C., Azulay, D., Pinto, J., Carneiro, S., and Dias, E. (2017). Investigation of the clinical features of geographic tongue: unveiling its relationship with oral psoriasis. Int. J. Dermatol. *56*, 421–427.

Rasmussen, J.E. (1986). Psoriasis in children. Dermatol. Clin. *4*, 99–106.

Raychaudhuri, S.K., Maverakis, E., and Raychaudhuri, S.P. (2014). Diagnosis and classification of psoriasis. Autoimmun. Rev. *13*, 490–495.

Reich, K., Krüger, K., Mössner, R., and Augustin, M. (2009). Epidemiology and clinical pattern of psoriatic arthritis in Germany: a prospective interdisciplinary epidemiological study of 1511 patients with plaque-type psoriasis. Br. J. Dermatol. *160*, 1040–1047.

Saleh, D., and Tanner, L.S. (2018). Psoriasis, Guttate. (StatPearls Publishing).

Schön, M.P., Boehncke, W.-H., and Bröcker, E.B. (2005). Psoriasis: Clinical manifestations, pathogenesis and therapeutic perspectives. Discov. Med. *5*, 253–258.

Seneschal, J., Milpied, B., and Taieb, A. (2012). Cutaneous drug eruptions associated with the use of biologies and cutaneous drug eruptions mimicking specific skin diseases. Chem. Immunol. Allergy *97*, 203–216.

Stankier, L. (1974). Diseases of the skin. Psoriasis. Br. Med. J. *1*, 27–29.

Stern, R.S. (1997). Psoriasis. Lancet *350*, 349–353.

Swabb, E.A., Wei, J., and Gullino, P.M. (1974). Diffusion and convection in normal and neoplastic tissues. Cancer Res. *34*, 2814–2822.

Talwar, S., Tiwari, V.D., Lakhtakia, R., and Panvelkar, V. (1995). Sequential clinico-histological studies in psoriasis following methotrexate therapy. Indian J. Dermatol. Venereol. Leprol. *61*, 284–287.

Whyte, H.J., and Baughman, R.D. (1964). Acute Guttate Ppsoriasis Aand Sstreptococcal Infection. Arch. Dermatol. *89*, 350–356.

Wollenberg, A., and Eames, T. (2011). Skin diseases following a Christmas tree pattern. Clin. Dermatol. *29*, 189–194.

Ziemer, M., Eisendle, K., and Zelger, B. (2009). New concepts on erythema annulare centrifugum: a clinical reaction pattern that does not represent a specific clinicopathological entity. Br. J. Dermatol. *160*, 119–126.